Journal of Volcanology and Geothermal Research 181 (2009) 115–123

Contents lists available at ScienceDirect

Journal of Volcanology and Geothermal Research

journal homepage: www.elsevier.com/locate/jvolgeores

Study of effect of magma pocket on mixing of two magmas with different viscosities and densities by analogue experiments

Eiichi Sato [a,*], Hiroaki Sato [b]

[a] Department of Earth and Planetary Sciences, Graduate School of Science and Technology, Kobe University, Rokkodai 1-1, Nada-ku, Kobe 657-8501, Japan
[b] Department of Earth and Planetary Sciences, Graduate School of Science, Kobe University, Rokkodai 1-1, Nada-ku, Kobe 657-8501, Japan

ARTICLE INFO

Article history:
Received 18 September 2008
Accepted 3 January 2009
Available online 14 January 2009

Keywords:
magma mixing
magma pocket
Rayleigh–Taylor instability
magma withdrawal

ABSTRACT

We conducted analogue experiments to examine the effect of a magma pocket on magma mixing processes at both high and low Reynolds numbers. Our idea is that when mafic and silicic magmas are simultaneously injected into a magma pocket, gravitationally unstable layers may be formed at both high and low Reynolds numbers. Under certain conditions, the Rayleigh–Taylor instability occurs and mixing of the two magmas is promoted in the pocket even at a low Reynolds number. This shows that gravitational force overcomes viscous force, and the annular flow of the magmas in the pocket is disrupted. If the viscous force is large, the annular flow is maintained, and it passes through the pocket. At a critical condition, two liquids with different densities and viscosities become unstable while mixing in the pocket. This condition is represented by a dimensionless parameter P ($P=\mu U/(g\Delta\rho ab/\pi)$), where μ is the viscosity, U is the flow velocity, g is the acceleration due to gravity, $\Delta\rho$ is the density difference between the two liquids, and a and b are the base dimensions of the apparatus. When $P<0.1$, the two liquids are gravitationally unstable and they mix in the pocket. However, when $P>0.1$, the annular flow of the two liquids is maintained, and they do not mix with each other. The critical condition is also dependent on the flux of the liquids and the height of the pocket, and is applicable to the present experimental conditions. The presence of the magma pocket is one of the factors responsible for the disruption of the annular flow, leading to the mixing of the two magmas. We conclude that magmas can mix thoroughly if they flow through several magma pockets.

1. Introduction

Bunsen (1851) was the first to recognize the importance of magma mixing as a petrogenetic process (Wilcox, 1999). Modern petrological methods have provided firm evidences of magma mixing in the mid-1970s (Eichelberger, 1975; Anderson, 1976; Sakuyama, 1979, 1981). These petrological studies were almost contemporaneous with the start of the application of fluid mechanics to magmatic processes, and promoted the study on the mechanism of magma mixing in the 1980s (Huppert et al., 1982; Koyaguchi, 1985; Turner and Campbell, 1986; Blake and Campbell, 1986; Freundt and Tait, 1986; Koyaguchi and Blake, 1989). These experimental studies clarified the conditions for mixing of magmas, whereas petrological studies indicated variable scales of mixing of magmas of multiple end components, whose thermodynamic properties have been examined by Sparks and Marshall (1986). Since the 1990s, mixing processes of magmas have been investigated by numerical calculations (Oldenburg et al., 1989; Bergantz and Breidenthal, 2001), petrological modeling (Murphy et al., 2000; Couch et al., 2001), and fractal analyses of natural samples (Wada, 1995; De Rosa et al., 2002; Perugini et al., 2003). Perugini et al. (2003) reported that repeated stretching and folding processes with element diffusion are necessary for producing variably mingled/mixed magmas.

The conditions under which magmas mix in a conduit have been determined by analogue experiments. In an open conduit system, where both inflow and outflow of magmas can occur, the instability of the annular flow of the magmas may cause mixing only at a high Reynolds number (Koyaguchi, 1985; Blake and Campbell, 1986; Freundt and Tait, 1986). However, in the case of effusive eruptions, the Reynolds numbers of the magmas in the conduit are generally low. For example, in the case of the dome-growth eruption of Mt. St. Helens, the Reynolds number of the magma in the conduit was less than 0.1 (Rutherford and Hill, 1993). This value is much smaller than the Reynolds numbers at which mixing occurs in a conduit ($Re>3$, Blake and Campbell, 1986; $Re>100$, Freundt and Tait, 1986). By using a closed, squeezed conduit, Koyaguchi and Blake (1989) investigated the conditions under which two magmas may mix within a rising magma batch at a low Reynolds number. Their results may be inadequate to model an open conduit system for steady-state effusion of mixed magmas. In this paper, we present the results of analogue experiments and explain the effect of a magma pocket on the mixing processes of magmas. We show that the presence of a magma pocket in a conduit

* Corresponding author. Tel.: +81 78 803 5732; fax: +81 78 803 5757.
E-mail address: esato@kobe-u.ac.jp (E. Sato).

0377-0273/$ – see front matter © 2009 Elsevier B.V. All rights reserved.
doi:10.1016/j.jvolgeores.2009.01.005

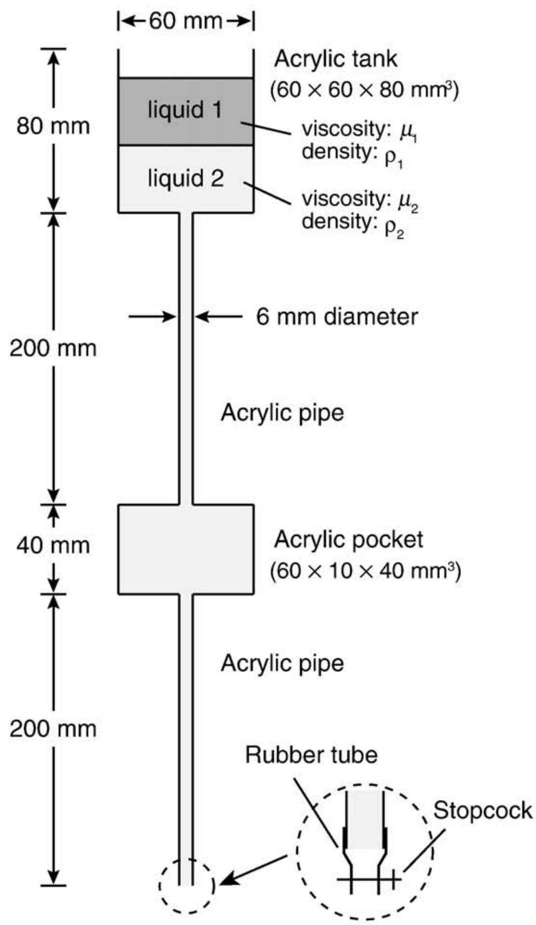

Fig. 1. Schematic diagram of the apparatus. We filled the tank with two liquids that satisfy the conditions $\mu_2 > \mu_1$ and $\rho_2 > \rho_1$. The sizes of the acrylic tank and pocket are expressed as follows: side × side × height.

causes an additional gravitational instability resulting in mingling/mixing of magmas even at a low Reynolds number.

2. Experimental method

We conducted analogue experiments using an acrylic apparatus to investigate the effect of a magma pocket. The main components of this apparatus were as follows: an upper tank with dimensions of 60 mm × 60 mm × 80 mm; a pipe with an inner diameter of 6 mm, outer diameter of 10 mm, and length of 200 mm; a pocket with dimensions of 60 mm × 10 mm × 40 mm; and another pipe with inner diameter of 6 mm, outer diameter of 10 mm, and length of 200 mm (Fig. 1). The first pipe was connected to both the tank and the pocket, and second pipe was connected only to the pocket. We attached a rubber tube with stopcock to the tip of the second pipe to prevent outflow of the two liquids before the experiments. First, we filled the pocket and the pipes with liquid 2 (dense, highly viscous, clear, and colorless). Then, we closed the stopcock and poured liquid 2 in the tank up to 10–30 mm thick. When the surface of liquid 2 stabilized, we poured liquid 1 (dyed liquid whose density and viscosity are lower than those of liquid 2) on it up to a height of 30 mm. Each experiment was started by opening the stopcock and allowing the liquids to flow downward under gravity. We assumed that liquids 1 and 2 correspond to mafic and silicic magmas, respectively. Our apparatus was inverted in comparison with the natural magma system. The differences in the density and viscosity of the two liquids were also opposite to those of magmas in the natural magma system; that is, the viscous liquid (liquid 2) was denser than the less viscous liquid (liquid 1). Consequently, in this study, we substituted the gravity effect of mafic magma in the natural magma system with the buoyancy effect of liquid 1. Eventually, our apparatus simulated the natural magma system, as in similar experimental studies (Koyaguchi, 1985; Blake and Campbell, 1986).

The liquids used to form the upper layer (liquid 1) and lower layer (liquid 2) were distilled water (density (ρ): 1000 kg/m^3, viscosity (μ): 0.001 Pa s), glue (polyvinyl alcohol–water) (ρ: 1020 kg/m^3, μ: 0.59 Pa s), syrup–water mixtures (ρ: 1340–1480 kg/m^3, μ: 0.56–150.3 Pa s), and glycerin–water mixtures (ρ: 1210–1250 kg/m^3, μ: 0.07–0.93 Pa s). The densities and viscosities of the syrup–water and glycerin–water mixtures vary with the water content according to the following equations (the numbers in parentheses indicate correlation coefficients): $\rho_{\mathrm{syrup}} = 1477 - 874A$ ($R = 0.989$), $\mu_{\mathrm{syrup}} = 0.0127A^{-2.27}$ ($R = 0.980$) for $A = 0.02 - 0.20$, $\rho_{\mathrm{glycerin}} = 1249 - 190A$ ($R = 0.994$), and $\mu_{\mathrm{glycerin}} = 0.0104A^{-1.16}$ ($R = 0.999$) for $A = 0.05 - 0.25$, where A denotes the weight fraction of water in each mixture. The experiments were conducted at approximately 24 °C.

Using video cameras (30 frames/s), we recorded the appearances of the liquids 1 and 2 in the tank and the pocket during the experiments in order to describe their textures and flow volumes (V_1 and V_2, respectively) in the tank. We also measured the apparent diameter of liquid 1 (D') in the pipe. We applied a refraction correction to the diameter of liquid 1 by using the following equation: $D_1 = D'/1.49$, where D_1 is the actual diameter of liquid 1 and 1.49 is the refractive index of acrylic resin (Appendix A). The refraction between the acrylic resin and the liquid was neglected. Consequently, we obtained the following parameters: velocity of liquid 1 in the first

Table 1
Experimental conditions

Experiment	Liquid 1			Liquid 2			Dimensionless parameter				Morphology of the liquid 1[a]
		ρ_1 (kg/m^3)	μ_1 (Pa s)		ρ_2 (kg/m^3)	μ_2 (Pa s)	ρ_2/ρ_1	μ_2/μ_1	Re_1	P	
1	Water	1000	0.001	Syrup–water	1330	0.56	1.33	560	171–558	0.023–0.058	F-spread
2	Glue	1020	0.59	Syrup–water	1390	2.76	1.36	4.68	0.078–0.26	0.022–0.083	F-lobe
3	Syrup–water	1330	0.56	Syrup–water	1390	2.76	1.06	4.93	0.039–0.13	0.083–0.15	O
4	Water	1000	0.001	Syrup–water	1390	2.76	1.39	2760	53–310	0.019–0.15	F-spread
5	Glue	1020	0.59	Syrup–water	1450	28.7	1.42	48.64	0.017–0.040	0.023–0.077	F-lobe
6	Water	1000	0.001	Glue	1020	0.59	1.02	590	171–763	0.54–1.81	O
7	Water	1000	0.001	Glycerin	1250	0.93	1.25	930	116–282	0.032–0.066	F-spread
8	Glycerin	1250	0.93	Syrup–water	1390	2.76	1.11	2.97	0.030–0.085	0.059–0.12	F-lobe
9	Syrup–water	1390	2.76	Syrup–water	1450	28.7	1.04	10.4	00.0019–0.0077	0.091–0.40	O
10	Glycerin–water	1210	0.067	Glycerin	1250	0.93	1.03	13.88	0.79–8.59	0.13–1.03	O, F-lobe

ρ_1 and ρ_2 are densities of liquid 1 and liquid 2, respectively. μ_1 and μ_2 are viscosities of liquid 1 and liquid 2, respectively.
ρ_2/ρ_1 and μ_2/μ_1 are density and viscosity ratios of liquid 1 and liquid 2, respectively.
Re_1 is the Reynolds number of liquid 1 in the first pipe. P is the dimensionless parameter (see text).
[a] Morphology of liquid 1 in the pocket. F-spread, F-lobe, and O represent the flotation shape (spread type), flotation shape (lobe type), and oblate-disk shape, respectively.

pipe: $U_1=[V_1(t_2)-V_1(t_1)]/[(t_2-t_1)(\pi D_1^2/4)]$ and Reynolds number of liquid 1 in the first pipe: $Re_1=D_1U_1\rho_1/\mu_1$. Here, $[V_1(t_2)-V_1(t_1)]$ represents the flow volume of liquid 1 from time (t_1) to time (t_2), and ρ_1 and μ_1 denote the density and viscosity of liquid 1, respectively.

3. Experimental results

We conducted 10 experiments; the experimental conditions are listed in Table 1. Fig. 2 shows some of the experimental results; the pictures

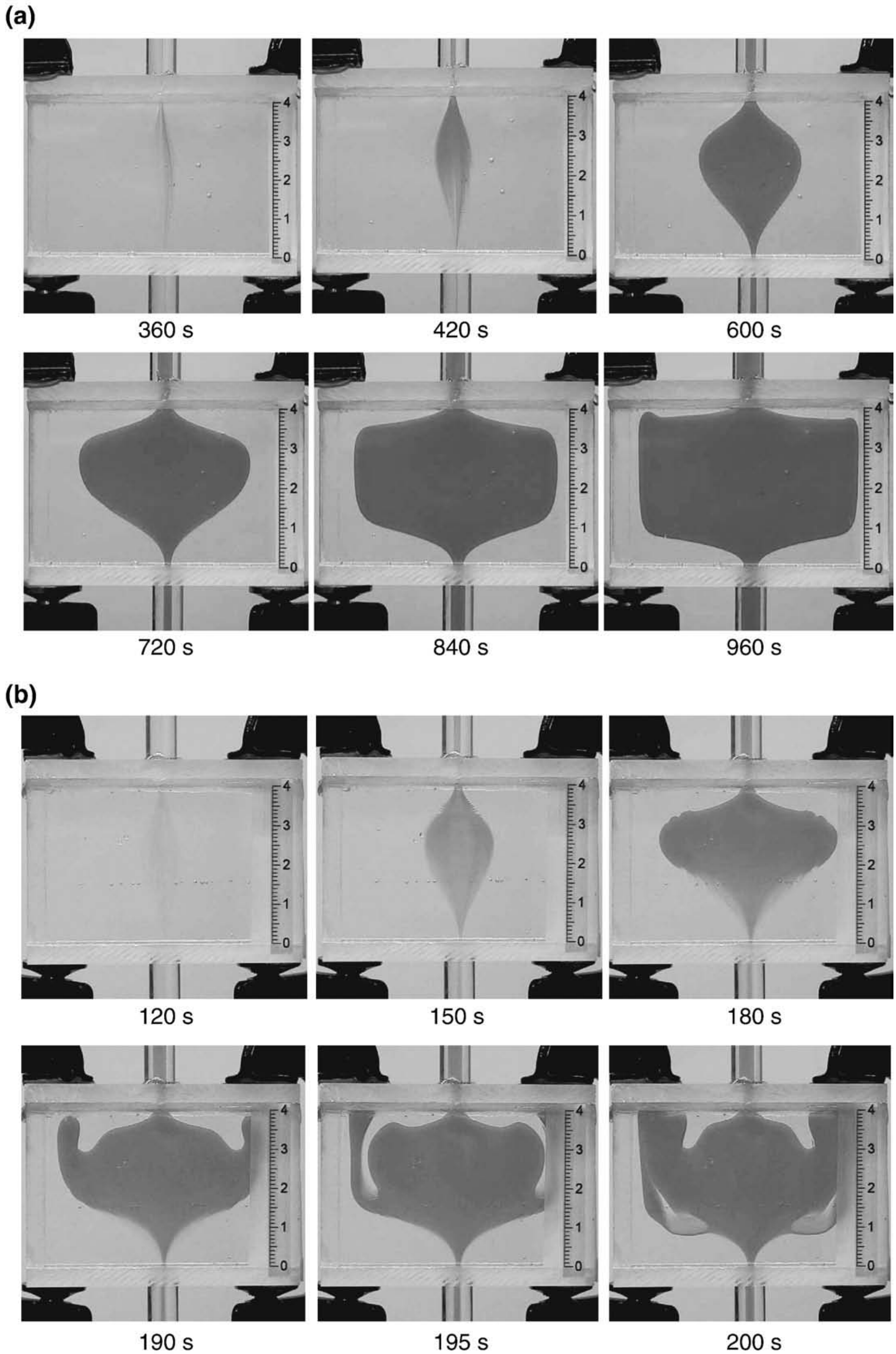

Fig. 2. Successive video images captured during experiments. (a) Oblate-disk shape (experiment 3). (b) Oblate-disk shape with flotation shape formed subsequently in the intermediate stage of the experiment (190–200 s) (experiment 10). (c) Flotation shape (spread type, experiment 1). (d) Flotation shape (lobe type, experiment 8).

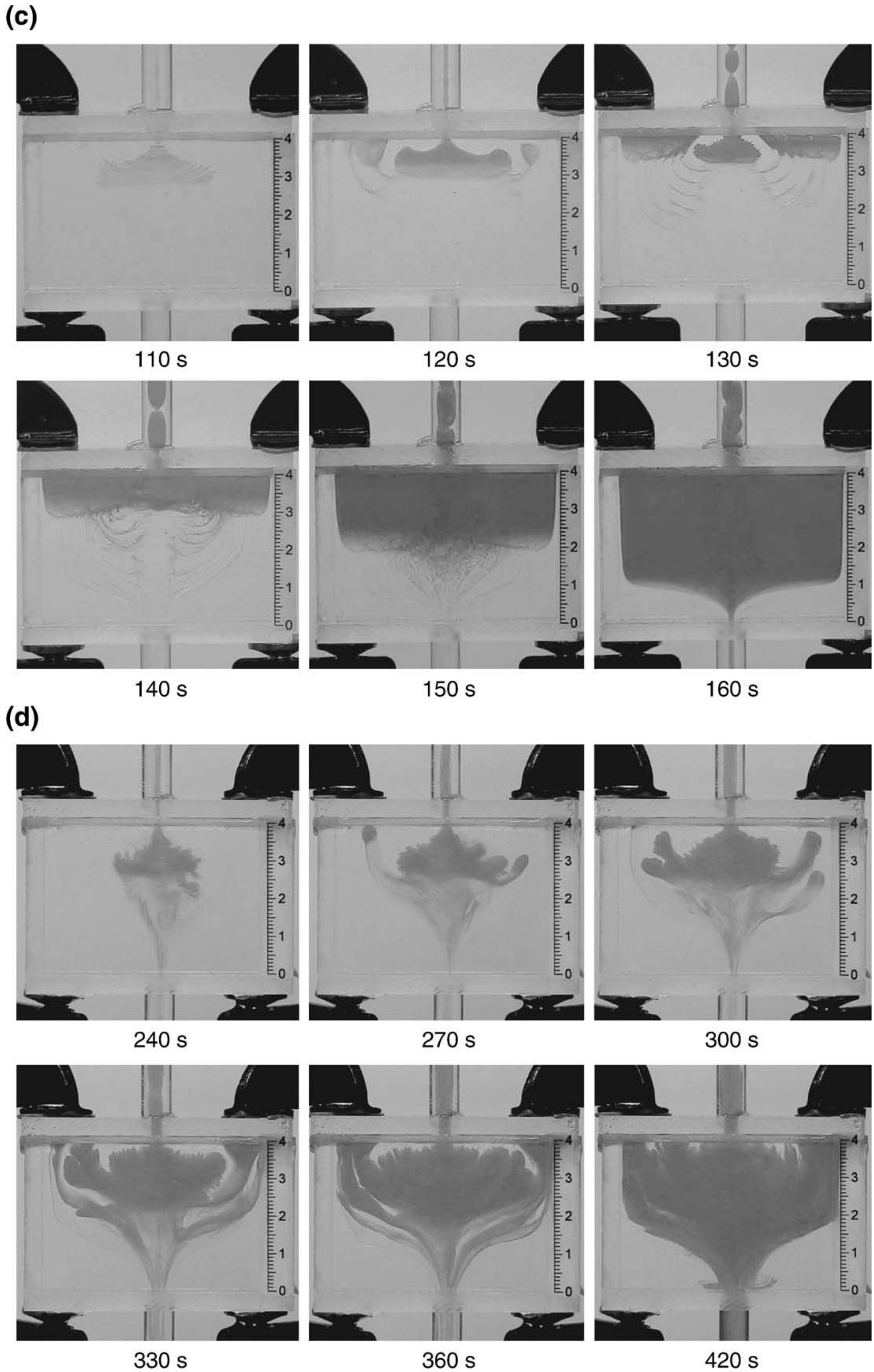

Fig. 2 (*continued*).

reveal the variation in the morphology of liquid 1 (dyed) in the pocket from the period of initial injection to the period of almost full occupancy in the pocket. Initially, only liquid 2 was drained from the tank into the first pipe, but subsequently, when the boundary of the two liquids fell to a critical depth (Blake and Ivey, 1986), liquid 1 was sucked into the first pipe through the center of liquid 2. Initially, a thin stream of liquid 1 entered the first pipe; over time, however, the thickness of the stream increased. Similarly, in the pocket, liquid 1 was first introduced as a thin streak, and its width increased with time. The time taken by liquid 1 to fill the pocket ranged from 60 s to 3000 s. We classified the morphologies of liquid 1 in the pocket into an oblate-disk shape and a flotation shape. The flotation shape was subdivided into two types (spread type and lobe type). The oblate-disk shape was observed in experiments 3, 6, and 9, whereas the flotation shape was observed in experiments 1, 4, and 7 (spread type) and 2, 5, and 8 (lobe type). In experiment 10, both the oblate-disk shape and flotation shape (lobe type) were observed.

3.1. Oblate-disk shape

Fig. 2(a) shows sequential pictures of the oblate-disk shape (experiment 3, Table 1). When liquid 1 was injected into the pocket, it flowed in the form of thin streams; thus, it exhibited the spindle morphology (Fig. 2(a) 360 s and 420 s). Generally, however, liquids 1 and 2 flowed continuously were clearly separated from each other. Liquid 1 initially exhibited a thread-like morphology; its thickness increased with time, and it finally exhibited the oblate morphology. Eventually, liquid 1 spread over the entire pocket, and the two liquids were sucked into the second pipe. As shown in Fig. 2 ((a) 960 s), the oblate disk of liquid 1 flows upward near the upper lateral ends of the oblate disk. This is because of the slight difference in the densities of the two liquids (liquid 1: 1330 kg/m^3, liquid 2: 1390 kg/m^3).

In experiment 10 (Fig. 2(b), Table 1), initially, liquid 1 formed a spindle morphology that developed into an oblate-disk shape (Fig. 2(b) 120–180 s), but subsequently, the peripheral end of liquid 1 floated and liquid 2 fell through liquid 1, where we could observe a lobate shape and stretching of liquid 1 (Fig. 2(b) 190–200 s). This shape is similar to the flotation shape (lobe type). Therefore, experiment 10 demonstrates the transition from the oblate-disk shape to the flotation shape.

3.2. Flotation shapes

3.2.1. Spread type

Fig. 2(c) shows sequential pictures of the flotation shape (spread type) (experiment 1, Table 1). When the two liquids were injected into the pocket, liquid 1 stagnated around the inlet of the pocket. Then, it spread laterally in the upper part of the pocket, and its peripheral ends floated to the ceiling of the pocket (Fig. 2(c) 120 s). Liquid 2 accumulated near the inlet of the pocket and intermittently flowed downward through the laterally spread liquid 1 as a spherical mass; while flowing downward, liquid 2 dragged and stretched liquid 1. At this time, liquid 1 was partly entrained by liquid 2, and the contact area between the two liquids increased significantly. These phenomena occurred repeatedly and alternate layers of liquids 1 and 2 were formed at the center of the pocket (Fig. 2(c) 130 s). Fig. 3 shows the formation of these layers in greater detail. The image captured at 112 s shows the situation just before the formation of the first layer of liquid 1 in the pocket. As shown in the image captured at 116 s, the first blob of colorless liquid 2 penetrated the first layer of liquid 1, and the second layer of liquid 1 was formed. Spreading of liquid 1 and downflow of liquid 2 occurred repeatedly and eventually resulted in the formation of four layers of liquid 1 between 112 s and 124 s.

A spread type is generally formed at a high Reynolds number (Re_1>50) in the first pipe (Table 1). Under these conditions, the annular flow in the first pipe may show a bead shape (Fig. 2(c) 130–160 s), similar to that observed by Blake and Campbell (1986). The entrance of the bead-shaped annular flow from the first pipe into the pocket formed the fine zig zag boundary of the two liquids in the upper part of pocket (Fig. 3, 112 s and 116 s). These phenomena also facilitate mixing of the two liquids.

3.2.2. Lobe type

In the experiments in which the lobe type was observed (experiment 8, Fig. 2(d), Table 1), the flotation of liquid 1 in the pocket was also observed, similar to the experiments in which a spread type was seen. However, in a lobe type, certain amounts of liquid 1 repeatedly floated to form lobes from the accumulated central broad column of liquid 1, which formed near the center of the pocket (Fig. 2(d) 270–330 s). Each liquid is contiguous in the lobe type. These morphologies differ from those of the spread type.

When the two liquids were injected into the pocket, liquid 1 aggregated at the center of the pocket. It was extruded horizontally

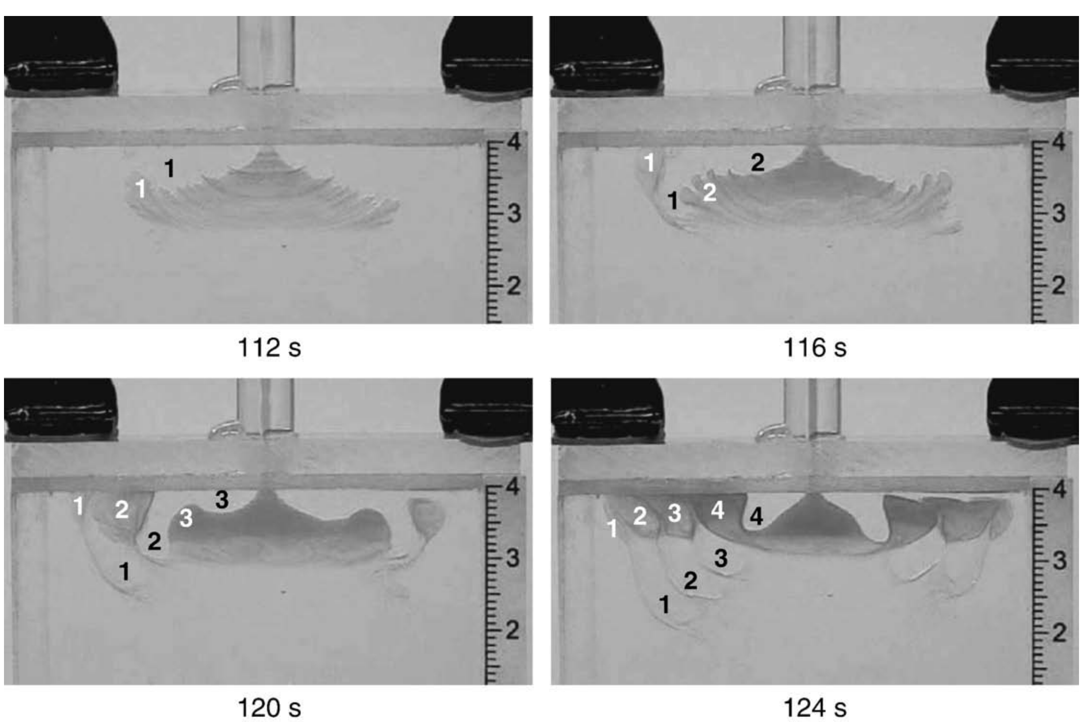

Fig. 3. Enlarged images showing the growth of alternate layers in the experiment in which a spread type was observed (experiment 1).

from the lower part of the aggregate to both sides in the form of lobes. Subsequently, the lobes deflected and floated upward to the ceiling of the pocket, while the lowest part of the aggregate was drawn into the second pipe (Fig. 2(d) 270 s). Thereafter, several lobes were repeatedly formed, and all of them floated upward. The formation of the lobes in the pocket is not necessarily symmetrical. Liquid 2 that was simultaneously injected into the pocket flowed downward and dragged and stretched liquid 1 (Fig. 2(d) 330 s). As shown in Fig. 2(d) (360 s and 420 s), a part of the aggregate of liquid 1 expanded and floated toward the ceiling of the pocket, whereas the remaining part was dragged into the second pipe.

4. Discussion

4.1. Mixing processes in the pocket

Our experiments demonstrated that the presence of a pocket in a conduit system might enhance the instability of the annular flow of two liquids with different densities. We classified the experimental results according to the shapes of liquid 1 in the pocket, i.e., oblate-disk shape and flotation shape (the latter was subdivided into spread type and lobe type). When the oblate-disk shape is formed, the two liquids remain separate and maintain the annular flow even when they are sucked into the second pipe (Fig. 2(a)); it appears that the two liquids do not mix in this case. On the other hand, when the flotation shape is formed, the two liquids form alternate layers or lobes, and the contact area increases with time; this indicates that mixing is promoted under these conditions (Fig. 2(c), (d)). In this section, we examine the formation processes of the alternate layers and lobes in the pocket and discuss the conditions under which the two liquids mix with each other.

The mixing processes in the pocket involve at least three basic fluid dynamical processes; i.e., mixing of the liquids during turbulent injection, Rayleigh–Taylor instability, and withdrawal of the liquids from the bottom of the pocket. The first and second processes have been discussed by Campbell and Turner (1986), and the third process has been discussed by Blake and Ivey (1986). We interpret our results on the basis of these processes.

Campbell and Turner (1986) determined the conditions under which magma mixing occurs in a magma chamber during replenishments. They found that when the Reynolds number of injected liquid 1 is large, the two liquids may mix in the chamber if they have similar viscosities. When the difference between the viscosities of the two liquids is large, mixing accompanied by the injection of less viscous liquid 1 is suppressed due to the high viscosity of liquid 2, even when the Reynolds number of liquid 1 is large (Fig. 4(a)). Our experiments were conducted under this condition, and mixing due to turbulent injection did not occur.

In the present experiments, liquids 1 and 2 were simultaneously injected into the pocket, and gravitationally unstable layers were inevitably formed in the upper part of the pocket (Fig. 4(b)). In general, when a dense liquid forms a layer on top of a less dense liquid, Rayleigh–Taylor instability may occur (Whitehead and Luther, 1975; Turcotte and Schubert, 2001). In the experiments in which the flotation shape was observed, liquid 1 floated through liquid 2 and was sandwiched between layers of liquid 2. Liquid 2 repeatedly flowed downward through layers of liquid 1; therefore, alternate stretched layers of the two liquids were produced at the center of the pocket

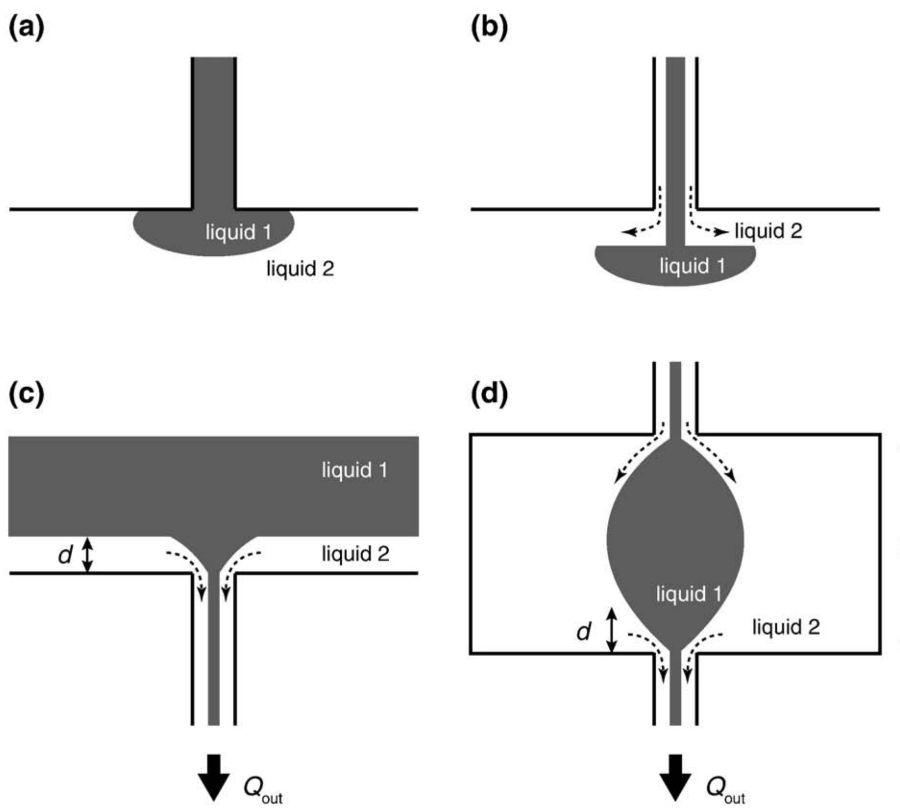

Fig. 4. Schematic figures of the previous and present experiments. (a) Experiment on magma mixing in a magma chamber conducted by Campbell and Turner (1986). When the difference between the viscosities of the two liquids is large, mixing is suppressed due to the high viscosity of liquid 2. (b) Present experiment. When the two liquids were simultaneously injected into the pocket, gravitationally unstable layers were inevitably formed in the upper part of the pocket. In the experiment in which the flotation shape was observed, liquid 1 floated through liquid 2, and liquid 2 flowed downward through liquid 1 due to the Rayleigh–Taylor instability (see Fig. 3). (c) Experiment of Blake and Ivey (1986). When the viscosity of liquid 2 is large, the two liquids are simultaneously sucked into the second pipe. (d) Experiment in which the oblate-disk shape was observed. The gravitationally unstable layer was formed in the upper part of the pocket, but liquid 1 was sucked into the second pipe due to the viscous force of liquid 2. Dashed arrows represent the flows of liquid 2.

(Fig. 3). The downflow of liquid 2 through the layers of liquid 1 may be dealt with by using the Stokes law. Whitehead and Luther (1975) presented the following equation for the Stokes approximation:

$$v = (\Delta\rho g a^2)/3\mu_2 \times [(\mu_2 + \mu_1)/(\mu_2 + (3/2)\mu_1)]$$

where v denotes the falling velocity; $\Delta\rho$, the density difference between the two liquids; g, the acceleration due to gravity; and a, the radius of spherical masses. We measured the velocities of liquid 2 as it flowed downward through the layers of liquid 1 in the spread type experiments; we also measured the rising velocity of the lobe in the lobe type experiments. These velocities were mostly consistent with the theoretical velocities, although the measured velocities are 1.1–1.2 times smaller than v. This difference may be ascribed to the friction effect of the pocket wall.

The gravitationally unstable layers were formed in all the experiments because the two liquids with different densities were simultaneously injected into the pocket (Fig. 4(b)). However, the Rayleigh–Taylor instability occurred only in the experiments in which the flotation shape was observed. The oblate-disk shape was formed when liquid 1 was sucked into the second pipe; hence, the withdrawal of liquid 1 from the pocket into the second pipe is a necessary condition for the formation of the oblate-disk shape. Blake and Ivey (1986) determined the conditions under which both the liquids are simultaneously evacuated from the bottom of the pocket (Fig. 4(c)). When the viscosity of liquid 2 was high, both the liquids were simultaneously sucked into the second pipe. They revealed the condition that was determined by the balance of viscous force (including the flux of the two liquids) and buoyancy force. In our experiments, when the viscous force of liquid 2 overcame the buoyancy force of liquid 1 at the bottom of the pocket, liquid 1 might be sucked into the second pipe, and the oblate-disk shape was formed (Fig. 4(d)). The conditions for the withdrawal of liquid 1 from the bottom of the pocket may also depend on the flux of the liquids (Q_{out}) and the critical drawn-down height (d) (Fig. 4(d)). In the experiments conducted by Blake and Ivey (1986), Q_{out} was constant. However, in our experiments, Q_{out} was time dependent, because Q_{out} depends on the dimensions and configuration of the apparatus, such as the relative sizes of the tank and the pocket, initial depth of the layers of liquids 1 and 2 in the tank, and the length of the first pipe. Thus, in our experiments, Q_{out} affected the withdrawal of liquid 1. Q_{out} and d are equally effective in the withdrawal conditions (Blake and Ivey, 1986). The effect of the depth of the pocket (h) should also be taken into account (Fig. 4(d)). If h is extremely small, liquid 1 may be injected into the second pipe even when the flotation shape is formed. On the other hand, if h is large, liquid 1 may float before liquid 1 reaches the critical drawdown height (d) even when the oblate-disk shape is formed.

The mechanism of mixing in the present experiments depends on the effects of both the gravitational instability in the upper part of the pocket and the withdrawal of liquid 1 from the bottom of the pocket, as discussed above. When the two liquids are simultaneously injected into the pocket, the gravitationally unstable layers are inevitably formed and the Rayleigh–Taylor instability occurs repeatedly. Alternate layers of the two liquids are formed, and the contact area increases significantly. However, when liquid 1 is sucked into the second pipe before the occurrence of the Rayleigh–Taylor instability, the gravitational instability may not occur.

We estimate the basic conditions for mixing of two liquids in fixed conditions of the present experiments. In order to evaluate the balance between the gravitational instability in the upper part of the pocket and the withdrawal of the liquids from the bottom of the pocket due to viscous force, we introduce a new dimensionless number P defined as

$$P = \mu_2 U_{ave}/(g\Delta\rho ab/\pi),$$

where μ_2 is the viscosity of liquid 2, U_{ave} is the average of the flow velocities of liquids 1 and 2, g is the acceleration due to gravity, $\Delta\rho$ is the density difference between the two liquids, and a and b are the base dimensions of the rectangular pocket. Fig. 5(a) and (b) show plots of P against Re_1 and μ_2/μ_1, respectively. The transition between the oblate-disk shape and the flotation shape occurs at approximately P=0.1. This result is almost independent of Re_1 and μ_2/μ_1 (Fig. 5(a) and (b)), and liquid 1 can float in the pocket even at a low Reynolds number. The conditions under which the two types of shapes, spread type and lobe type, are formed seem to be related to the Reynolds number and ratio of viscosities. When the viscosity of liquid 1 in the pocket is low and its Reynolds number is high, it may spread laterally in the upper part of the pocket; however, when it has a high viscosity and a low Reynolds number, it is sustained in the pocket by the viscous force, but is eventually deflected due to gravity to form a lobe shape. Thus, the difference between the two types may depend on the Reynolds number and ratio of viscosities. When Re_1 and μ_2/μ_1 are larger than 10 and 500, respectively, the spread type is observed. However, when Re_1 and μ_2/μ_1 are less than 1 and 50, respectively, the lobe type is observed in the pocket.

The expression of P is similar to that of the dimensionless parameter I defined by Koyaguchi and Blake (1989):

$$I = \mu_2 U/(g\Delta\rho r^2),$$

where U is the flow velocity and r is the radius of the pipe. However, P is essentially different from I. I represents the balance between the driving viscous force for circulation and the gravity force for suppression. The two liquids mix when I>0.1; under this condition, the predominance of viscous force over gravitational force generates cyclic overturn of the two liquids. In contrast, P represents the balance between the generation of gravitational instability in the upper part of the pocket and the

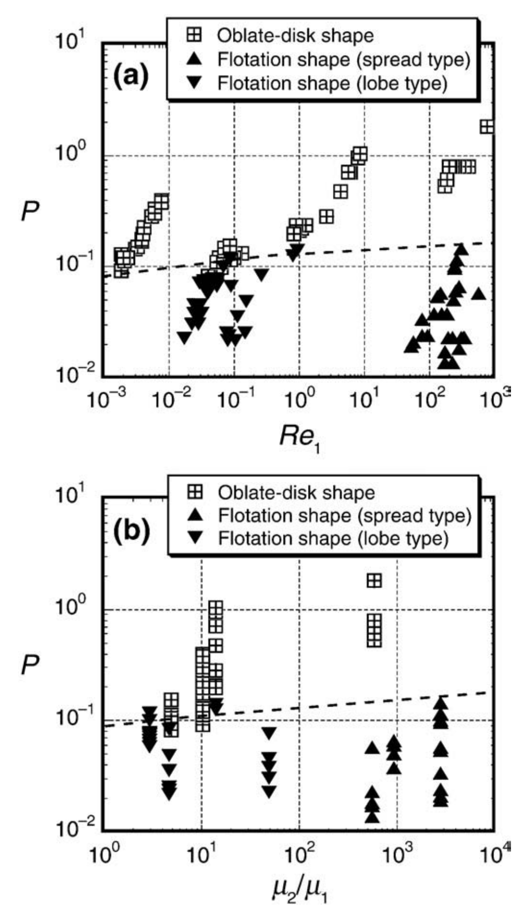

Fig. 5. (a) Plot of P against Re_1 for all experiments. (b) Plot of P against μ_2/μ_1 for all experiments. Dashed lines represent the boundary between the oblate-disk shape and the flotation shape. These lines correspond to approximately P=0.1.

withdrawal of the liquids from the bottom of the pocket due to viscous force. Because of these differences, the mixing condition for the present experiments is opposite to that determined by Koyaguchi and Blake (1989).

The results shown in Fig. 5 depend on *d* and *h*. The mixing condition ($P<0.1$) is applicable only to the present experiments. Additional experiments with different values of *d* and *h* may be necessary to determine the general implications. However, we suggest that the mixing condition *P* may be qualitatively applied to natural magmatic systems.

4.2. Geological application

We examined the effect of a magma pocket on the mixing process of two magmas and found that the presence of the magma pocket may enhance the mixing process. In this section, we discuss the effect of magma pockets in the case of the 1991–1995 eruption at Mt. Unzen, in relation to the present experimental results.

Mixing of two magmas in dome-forming eruptions generally occurs at very low Reynolds numbers. For example, the 1991–1995 dome-forming eruption of Unzen volcano, which had an open conduit system and erupted mixed dacite. The initial dome growth occurred at 3×10^5 m^3/day (Nakada et al., 1999), corresponding to 3.5 m^3/s. By assuming that the initial conduit diameter is 5–20 m (Noguchi et al., 2008), the average rising velocity is calculated to be 0.011–0.18 m/s, and the Reynolds number calculated on the basis of the density and viscosity of high-T magma is 0.21–0.86. In this case, we estimated the initial densities (high-T magma: 2400–2420 kg/m^3; low-T magma: 2370–2390 kg/m^3) and viscosities (high-T magma: $10^{3.4}$ Pa s; low-T magma: $10^{5.1}$ Pa s) of magmas by means of the analyzed chemical compositions of melt inclusions in phenocrysts and estimated end-member magmas (Holtz et al., 2005). The time scale of magma mixing at the Unzen volcano determined by using diffusion profiles of titanomagnetite indicated that there was short time interval between mixing and extrusion throughout the 1991–1995 eruption (ca 1 month: Nakamura, 1995). Thus, mixing of magmas may have occurred in the conduit. In the case of the Unzen volcano, four magma pockets were estimated (A: 0.6–1.3 km; B: 4.0 km; C: 6.8–7.0 km; and D: 15.0 km) by repeated leveling surveys and GPS measurements (Hendrasto et al., 1997; Kohno et al., 2008). The lowest chamber D may be the source of the high-T mafic magma, whereas the C pocket is considered to be the source of the low-T silicic magma (Venezky and Rutherford, 1999; Holtz et al., 2005). Therefore, the two magmas passed through at least two magma pockets (A and B) as they rose from the magma chamber to the surface. Using the inflation volume ($\Delta V=2.75\times10^6$ m^3) of the pocket (Hendrasto et al., 1997), we estimated that the diameter of the pocket at a depth of 4 km was more than 170 m. When the magmas were injected into pocket B at the depth of 4 km, the value of P_{pocket} of the magmas was less than 0.002–0.04. These values are lower than the value at which magma mixing occurs in the pocket and are much less than P_{conduit} (0.16–42.5). Thus, magma mixing may have been promoted by the presence of the magma pocket. We considered the changes in the initial densities and viscosities of the magmas when we calculated P_{pocket} and P_{conduit}. At a depth of 4 km, the initial H_2O contents of the high-T magma (ca. 4 wt.%, Holtz et al., 2005) and low-T magma (ca. 8 wt.%, Holtz et al., 2005) exceeded their water solubilities (Holtz et al., 1995). As a result, undissolved water may have formed bubbles, and the initial densities and viscosities of the high-T magma changed to 2200–2220 kg/m^3 and $10^{3.6}$ Pa s, while those of the low-T magma changed to 1940–1950 kg/m^3 and $10^{6.6}$ Pa s, respectively. In the case of the Unzen volcano, the extruded lavas exhibit uniform chemical compositions (Nakada and Motomura, 1999). Therefore, the mixing ratio of different magmas is almost constant during the period of effusion. However, in our study, the mixing ratio of liquid 1 abruptly increased at the end of the experiments due to the depletion of liquid 2 in the tank. We suggest that the effusion of lavas from the Unzen volcano corresponds to the intermediate stage of the experiments.

In an actual magma system, two end-member magmas have different liquidus temperatures, which may affect their mixing processes (Sparks and Marshall, 1986; Koyaguchi, 1986a,b). If the two magmas flow into a conduit and a pocket, the low-viscosity and high-T magma is locally cooled near the interface and its viscosity increases, whereas the high-viscosity and low-T magma is locally heated near the interface and becomes less viscous. Such transient conditions may cause complex distributions of the viscosities and densities of the two magmas, which may also cause flow instability, resulting in the mixing of the two magmas.

5. Concluding remarks

We conducted analogue experiments to examine the effect of a magma pocket on magma mixing processes in a conduit. The experiments showed that liquid 1 exhibited two morphologies in the pocket, oblate-disk shape and flotation shape; the flotation shape was further divided into two types (spread type and lobe type). The differences in the morphologies can be attributed to the balance between the Rayleigh–Taylor instability in the upper part of the pocket and withdrawal of the two liquids from the bottom of the pocket. When the two liquids were simultaneously injected into the pocket, gravitationally unstable layers were inevitably formed. When the oblate-disk shape was observed, withdrawal of liquid 1 from the bottom of the pocket occurred before the Rayleigh–Taylor instability, the two liquids maintained the annular flow in the second pipe and did not mix with each other. However, when the Rayleigh–Taylor instability occurred before the withdrawal of liquid 1, alternate layers of the two liquids were formed, and mixing was promoted in the pocket, even when the Reynolds number was low. We identified the transition between the flotation shape and the oblate-disk shape, using dimensionless number *P*, which is applied to conditions of the present experiments. The transition boundary appeared at approximately $P=0.1$. In the case of $P>0.1$, liquid 1 exhibited the oblate-disk shape, and liquids 1 and 2 did not mix with each other. However, in the case of $P<0.1$, liquid 1 formed a flotation shape, and the two liquids mixed even when the Reynolds number of liquid 1 was low.

Mafic and silicic magmas simultaneously ascending from a density-stratified magma chamber may form unstable layers and may mix together in the magma pocket. The magma pocket may be one of the important factors that promote mixing of magmas in a conduit.

Acknowledgments

We are grateful to Dr. K. Suzuki-Kamata and Dr. K. Yamasaki of Kobe University and Dr. K. Wada of Hokkaido University of Education for the useful comments and discussions. We also thank Mr. K. Sangen for helping in the development of the apparatus. We are much indebted to Dr. T. Koyaguchi for the thoughtful comments, which improved the content of the manuscript. This study was partly supported by the Sasakawa Scientific Research Grant and the Earthquake Research Institute cooperative research program B offered to E. S. and a grant-in-aid from JSPS awarded to H. S.

Appendix A

We measured the apparent diameter (D') of liquid 1 in the pipe. Its actual diameter (D_1) is obtained by dividing the apparent diameter by the refractive index of the acrylic pipe. In this calculation, we neglected the difference between the refractive indices of the acrylic resin and liquid 2. Fig. A1 shows the refraction of the light originating from the boundary between liquid 1 and liquid 2. D' and D_1 are equivalent to $D_{\mathrm{p}}\sin(\theta)$ and $D_{\mathrm{p}}\sin(i)$, respectively, where D_{p} represents the outer

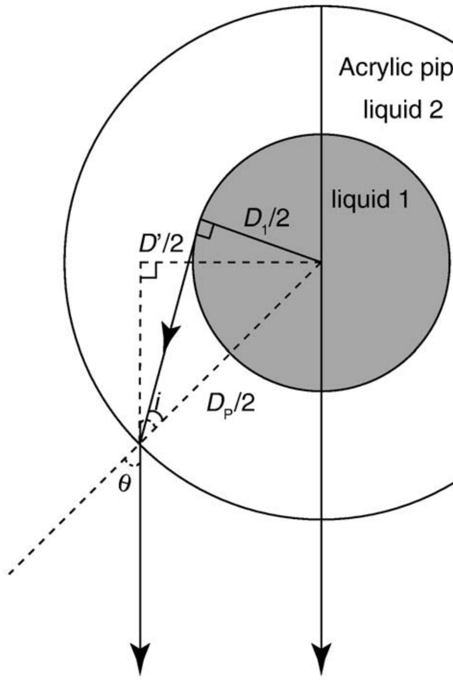

Fig. A1. Refraction of light originating from the boundary between liquids 1 and 2. D_1, D', and D_p represent the actual diameter, apparent diameter of liquid 1, and outer diameter of the pipe, respectively.

diameter of the acrylic pipe. Because $\sin(\theta)/\sin(i)$ = refractive index of the acrylic pipe (1.49), the true diameter is equal to $D'/1.49$.

References

Anderson, A.T., 1976. Magma mixing: petrological process and volcanological tool. J. Volcanol. Geotherm. Res. 1, 3–33.

Bergantz, G.W., Breidenthal, R.E., 2001. Non-stationary entrainment and tunneling eruptions: a dynamic link between eruption processes and magma mixing. Geophys. Res. Lett. 28, 3075–3078.

Blake, S., Campbell, I.H., 1986. The dynamics of magma-mixing during flow in volcanic conduits. Contrib. Mineral. Petrol. 94, 72–81.

Blake, S., Ivey, G.N., 1986. Magma-mixing and the dynamics of withdrawal from stratified reservoirs. J. Volcanol. Geotherm. Res. 27, 153–178.

Bunsen, R.W., 1851. Uber die processe der vulkanischen Gesteinsbildungen Islands. Ann. Phys. Chem. 83, 197–272.

Campbell, I.H., Turner, J.S., 1986. The influence of viscosity on fountains in magma chambers. J. Petrol. 27, 1–30.

Couch, S., Sparks, R.S.J., Carroll, M.R., 2001. Mineral disequilibrium in lavas explained by convective self-mixing in open magma chambers. Nature 411, 1037–1039.

De Rosa, R., Donato, P., Ventura, G., 2002. Fractal analysis of mingled/mixed magmas: an example from the Upper Pollara eruption (Salina Island, southern Tyrrhenian Sea, Italy). Lithos 65, 299–311.

Eichelberger, J.C., 1975. Origin of andesite and dacite: evidence of mixing at Glass Mountain in California and at other circum-Pacific volcanoes. Geol. Soc. Amer. Bull. 86, 1381–1391.

Freundt, A., Tait, S., 1986. The entrainment of high-viscosity magma into low-viscosity magma in eruption conduits. Bull. Volcanol. 48, 325–339.

Hendrasto, M., Eto, T., Kimata, F., Matsushima, T., Ishihara, K., 1997. Magma transport at Mt. Unzen associated with the 1990–1995 activity inferred from leveling data. Annuals, Disas. Prev. Res. Inst., Kyoto Univ. 40 (B-1), 61–72.

Holtz, F., Behrens, H., Dingwell, D.B., Johannes, W., 1995. H_2O solubility in haplogranitic melts: compositional, pressure, and temperature dependence. Am. Mineral. 80, 94–108.

Holtz, F., Sato, H., Lewis, J., Behrens, H., Nakada, S., 2005. Experimental petrology of the 1991–1995 Unzen dacite, Japan. part I: phase relations, phase composition and pre-eruptive conditions. J. Petrol. 46, 319–337.

Huppert, H.E., Sparks, R.S.J., Turner, S., 1982. Effects of volatiles on mixing in calc-alkaline magma systems. Nature 297, 554–557.

Kohno, Y., Matsushima, T., Shimizu, H., 2008. Pressure sources beneath Unzen Volcano inferred from leveling and GPS data. J. Volcanol. Geotherm. Res. 175, 100–109.

Koyaguchi, T., 1985. Magma mixing in a conduit. J. Volcanol. Geotherm. Res. 25, 365–369.

Koyaguchi, T., 1986a. Textural and compositional evidence for magma mixing and its mechanism, Abu volcano group, Southwestern Japan. Contrib. Mineral. Petrol. 93, 33–45.

Koyaguchi, T., 1986b. Evidence for two-stage mixing in magmatic inclusions and rhyolitic lava domes on Niijima island, Japan. J. Volcanol. Geotherm. Res. 29, 71–98.

Koyaguchi, T., Blake, S., 1989. The dynamics of magma mixing in a rising magma batch. Bull. Volcanol. 52, 127–137.

Murphy, M.D., Sparks, R.S.J., Barclay, J., Carroll, M.R., Brewer, T.S., 2000. Remobilization of andesite magma by intrusion of mafic magma at the Soufriere Hills Volcano, Montserrat, West Indies. J. Petrol. 41, 21–42.

Nakada, S., Motomura, Y., 1999. Petrology of the 1991–1995 eruption at Unzen: effusion pulsation and groundmass crystallization. J. Volcanol. Geotherm. Res. 89, 173–196.

Nakada, S., Shimizu, H., Ohta, K., 1999. Overview of the 1990–1995 eruption at Unzen Volcano. J. Volcanol. Geotherm. Res. 89, 1–22.

Nakamura, M., 1995. Continuous mixing of crystal mush and replenished magma in the ongoing Unzen eruption. Geology 23, 807–810.

Noguchi, S., Toramaru, A., Nakada, S., 2008. Relation between microlite textures and discharge rate during the 1991–1995 eruptions at Unzen, Japan. J. Volcanol. Geotherm. Res. 175, 141–155.

Oldenburg, C.M., Spera, F.J., Yuen, D.A., Sewell, G., 1989. Dynamic mixing in magma bodies: theory, simulations and implications. J. Geophys. Res. 94, 9215–9236.

Perugini, D., Poli, G., Mazzuoli, R., 2003. Chaotic advection, fractals and diffusion during mixing of magmas: evidence from lava flows. J. Volcanol. Geotherm. Res. 124, 255–279.

Rutherford, M.J., Hill, P.M., 1993. Magma ascent rates from amphibole breakdown: an experimental study applied to the 1980–1986 Mount St. Helens eruptions. J. Geophys. Res. 98, 19667–19685.

Sakuyama, M., 1979. Evidence of magma mixing: petrological study of Shirouma-Oike calc-alkaline andesite volcano, Japan. J. Volcanol. Geotherm. Res 5, 179–208.

Sakuyama, M., 1981. Petrological study of the Myoko and Kurohime volcanoes, Japan: crystallization sequence and evidence for magma mixing. J. Petrol. 22, 553–583.

Sparks, R.S.J., Marshall, L.A., 1986. Thermal and mechanical constraints on mixing between mafic and silicic magmas. J. Volcanol. Geotherm. Res. 29, 99–124.

Turcotte, D.L., Schubert, G.S., 2001. Geodynamics, 2nd Edition. Cambridge University Press, New York. 456 pp.

Turner, J.S., Campbell, I.H., 1986. Convention and mixing in magma chambers. Earth Sci. Rev. 23, 255–352.

Venezky, D.Y., Rutherford, M.J., 1999. Petrology and Fe–Ti oxide reequilibration of the 1991 Mount Unzen mixed magma. J. Volcanol. Geotherm. Res. 89, 213–230.

Wada, K., 1995. Fractal structure of heterogeneous ejecta from the Me-akan volcano, eastern Hokkaido, Japan: implications for mixing mechanism in a volcanic conduit. J. Volcanol. Geotherm. Res. 66, 69–79.

Whitehead, J.A., Luther, D.S., 1975. Dynamics of laboratory diapir and plume models. J. Geophys. Res. 80, 705–717.

Wilcox, R.E., 1999. The idea of magma mixing: history of a struggle for acceptance. J. Geol. 107, 421–432.